

g -factor measurement of the 2738 keV isomer in ^{135}La Md. S. R. Laskar,¹ S. Saha,¹ R. Palit,¹ S. N. Mishra,¹ N. Shimizu,² Y. Utsuno,^{2,3} E. Ideguchi,⁴ Z. Naik,⁵ F. S. Babra,¹ S. Biswas,¹ S. Kumar,⁶ S. K. Mohanta,¹ C. S. Palshetkar,¹ P. Singh,¹ and P. C. Srivastava⁷¹*Department of Nuclear and Atomic Physics, Tata Institute of Fundamental Research, Mumbai 400005, India*²*Center for Nuclear Study, The University of Tokyo, Hongo, Bunkyo-ku, Tokyo 113-0033, Japan*³*Advanced Science Research Center, Japan Atomic Energy Agency, Tokai, Ibaraki 319-1195, Japan*⁴*Research Center for Nuclear Physics (RCNP), Osaka University, Ibaraki, Osaka 567-0047, Japan*⁵*Sambalpur University, Sambalpur-768019, India*⁶*University of Delhi, Delhi-110007, India*⁷*Department of Physics, Indian Institute of Technology, Roorkee 247667, India*

(Received 30 July 2018; revised manuscript received 30 November 2018; published 9 January 2019)

The g factor of an isomeric state at 2738 keV in ^{135}La has been measured by time differential perturbed angular distribution technique. This isomer was populated in the reaction $^{128}\text{Te}(^{11}\text{B}, 4n)^{135}\text{La}$ at beam energy of 52 MeV. We performed the large-scale shell-model (LSSM) calculations which successfully describe the low-lying levels and band structures of ^{135}La . The measured value of the g factor, $-0.049(3)$, has been compared with the LSSM result to firmly assign the configuration of the isomeric state. The major configuration of $23/2^+$ state is $\pi(d_{5/2}) \otimes \nu(h_{11/2})^{-2}$.

DOI: [10.1103/PhysRevC.99.014308](https://doi.org/10.1103/PhysRevC.99.014308)**I. INTRODUCTION**

A number of high-spin isomers have been reported in nuclei around $A \approx 135$ with neutron number close to $N = 82$ shell closure, which have simple multiquasiparticle configurations [1–11]. These relatively pure states at high spin attract lot of theoretical attention as they can be directly related to shell-model configurations. The systematics of isomers in $N = 78$ and $N = 80$ have been reported in Refs. [11–17]. For even-even nuclei in this region, states with multiquasiparticle configurations based on $(\nu h_{11/2})^2$ and $\nu h_{11/2}(s_{1/2}d_{3/2})^1$ have been reported as yrast and can often have longer lifetime. It is interesting to explore the role of these two configurations when coupled with an odd particle (neutron or proton) in different orbitals for the generation of pure states at high spin in neighboring even-odd and odd-even nuclei, which can be an isomer. Recently, high-spin isomers have been reported in ^{139}Nd (even-odd) and ^{135}La (odd-even) [10,11]. In certain situations for odd- A nuclei, different multiquasiparticle configurations can energetically compete, which can give rise to uncertainty in the assignment of configurations for the isomers. In this context, further investigations are required for the determination of the configuration for the 2738 keV isomer in ^{135}La , which was assigned a spin-parity of $(23/2^+)$ recently in Ref. [10].

A 3-quasiparticle configuration $\pi h_{11/2} \otimes \nu h_{11/2}(s_{1/2}/d_{3/2})^1$ has been suggested for this isomer in ^{135}La [10]. From the angular-momentum algebra, the two appropriate configurations for the $23/2^+$ state are (i) ^{134}Ba (7^-) coupled to a proton in $0h_{11/2}$ and (ii) ^{134}Ba (10^+) coupled to proton in $(1d_{5/2}$ or $0g_{7/2})$. The difference of the experimental excitation energies between 7^- and 10^+ states of ^{134}Ba is -686 keV, while that of the proton $0h_{11/2}$ and $1d_{5/2}$ is simply estimated

to be 786 keV from the experimental excitation energy of $11/2^-$ in ^{135}La with respect to the $5/2^+$ state. These values are almost canceled, and the two couplings can compete with each other. For such cases, g -factor measurements are essential for the firm assignment of the configurations. The g factor of the 2738 keV isomer in ^{135}La has been tabulated to be $0.0(0.2)$ with an assigned spin of $(27/2^+)$ [18]. The details of the original measurement can be found in Ref. [19], where the g factor of the 2738 keV state with assigned spin of $(27/2^+)$ has been reported as $0.003(0.015)$. The isomer was produced in $^{133}\text{Cs}(\alpha, 2n)^{135}\text{La}$ reaction and the decaying γ rays from the states below the isomer in the external magnetic field were detected in NaI(Tl) detector. However, certain experimental details such as the value of the external magnetic field and the observed Larmor frequency were not mentioned in Ref. [19]. In a more recent work, Bansal *et al.* [20] measured the magnetic hyperfine interaction of ^{135}La recoil-implanted into ferromagnetic Fe host using La(Ce)Br₃ detectors. They used the hyperfine field (HF) of La in Fe to be $-22(5)$ T and deduced the g factor of the $23/2^+$ state at 2738 keV to be $0.11(2)$. Using NMR-ON technique, Goto *et al.* [21] have independently measured the hyperfine field of ^{140}La in Fe and reported it to be $-47(1)$ T. Because of the large discrepancy in the HF value of La in Fe, the derived g factor becomes highly uncertain. It is therefore important to measure the g factor with precisely known value of the magnetic field that can be applied from an external source like a superconducting magnet.

In this work, we present precision measurement of g factor for the 2738 keV, $23/2^+$ isomer in ^{135}La using time differential perturbed angular distribution (TDPAD) technique with a superconducting magnet. The measured g factor has

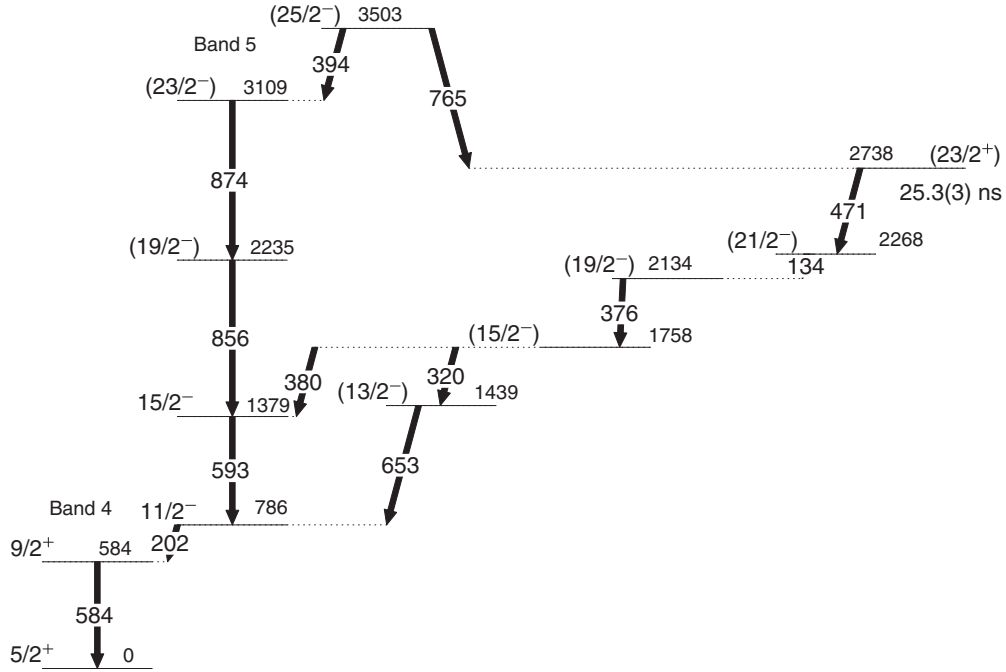


FIG. 1. Partial level scheme of ^{135}La showing the isomer at 2738 keV. The energies of the levels and the transitions have been marked in keV (adopted from Ref. [10]).

been compared with the results of the large-scale shell-model calculations to assign the configuration of the isomer.

II. EXPERIMENTAL DETAILS

The isomer at 2738 keV in ^{135}La was populated in the reaction $^{128}\text{Te}(^{11}\text{B}, 4n)^{135}\text{La}$ using pulsed ^{11}B beam at beam energy of 52 MeV provided by the heavy-ion accelerator facility at TIFR, Mumbai. An isotopically enriched 1 mg/cm^2 ^{128}Te was evaporated on 3.5 mg/cm^2 Au backing. Each beam pulse had a width of about 1 ns and the separation between the consecutive beam bunches was 800 ns. ^{135}La produced in the reaction was implanted in the Au backing. In the present experiment we have applied transverse magnetic field of 5 T, produced by a split coil superconducting magnet with field stability of better than 0.1% and uniformity of 0.5% over a spherical volume of $\approx 1\text{ cm}^3$. The field direction was reversed in every 6 hours. This setup has been regularly used to investigate magnetic properties of materials and study of hyperfine interactions using TDPAD technique [22–24]. The delayed γ rays from the 2738 keV isomer were measured by large volume ($\approx 143\text{ cm}^3$) HPGe detectors with relative efficiency of 30% with respect to a 3×3 inch NaI(Tl) scintillation detector. The detectors were placed at a distance of 11 cm from the target center at angles $\pm 45^\circ$ and $\pm 135^\circ$ with respect to the beam direction. The time resolution of the detectors was measured to be 5 ns at γ energy of 1332 keV of the standard ^{60}Co radioactive source. The time signal from the HPGe detector was used to start the time to amplitude converter (TAC), which was stopped by the primary RF signal of the buncher. The data were collected in LIST mode with eight parameters for energy and time signals for four detectors. In the offline analysis, two dimensional spectra with energy versus time

were constructed for each detector. The lifetime spectra for the γ rays decaying from the isomeric state were generated by taking energy gated time projections. Normalized counts for each detector $N(\theta, t)$ were used to construct the spin rotation spectra defined as

$$R(t) = [N \uparrow(\theta, t) - N \downarrow(\theta, t)] / [N \uparrow(\theta, t) + N \downarrow(\theta, t)]. \quad (1)$$

The spectra were fitted to the function

$$R(t) = -\frac{3}{4} A_2 \sin(2\omega_L t - \phi) \exp(-\lambda t) \quad (2)$$

to extract the amplitude A_2 , Larmor frequency ω_L , and damping factor λ . Here, ϕ denotes a phase angle due to finite bending of the incoming beam in external magnetic field. A fit of our experimentally observed $R(t)$ spectra to Eq. (2) yielded the value for ϕ to be $\approx 12(5)^\circ$.

III. RESULTS AND DISCUSSION

A. Experimental results

The partial level scheme of ^{135}La showing the decay of isomer is shown in Fig. 1. The delayed γ transitions from the isomer at 2738 keV excitation energy is shown in Fig. 2. Inset of Fig. 2 shows the lifetime decay spectrum obtained with energy gate on the 471 keV γ line. This was fitted with an exponential curve yielding a half-life ($T_{1/2}$) of 25.3(3) ns which is close to the reported value in Ref. [25] as well as the result of the centroid shift method (CSM) reported in Ref. [10]. However, our measured $T_{1/2}$ is slightly smaller compared to the value of 28.4(8) ns reported from PPAC- γ time difference spectrum in Ref. [10]. The time spectra generated with 471 and 376 keV transitions were used to form the

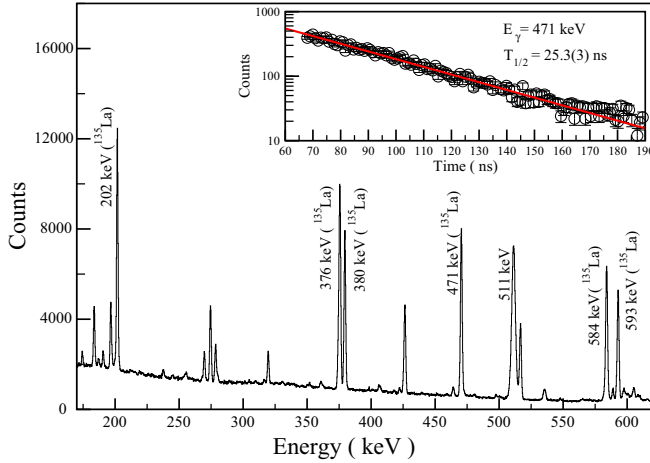


FIG. 2. Delayed γ spectrum showing the different transitions of ^{135}La . This spectrum is generated by putting a time gate of width 30 ns which is delayed by 30 ns from the prompt. Decay curve for the 471 keV transition showing the lifetime of the isomer in ^{135}La is given in the inset.

experimental modulation ratio $R(t)$. The experimental ratio functions and the corresponding least square fitted spectra are depicted in Fig. 3. The spectra fitted to the Eq. (2) yielded $\omega_L = 11.30(1.13)$ Mrad/s and $12.4(1.2)$ Mrad/s for 471 and 376 keV transitions, respectively. These provide the g factor of the $(23/2^+)$ isomer in ^{135}La as $-0.047(4)$ and $-0.052(5)$, giving a mean value of $-0.049(3)$. Our measured value of the g factor is close to the value quoted in Ref. [18], but in variance with the results reported by Bansal *et al.* [20].

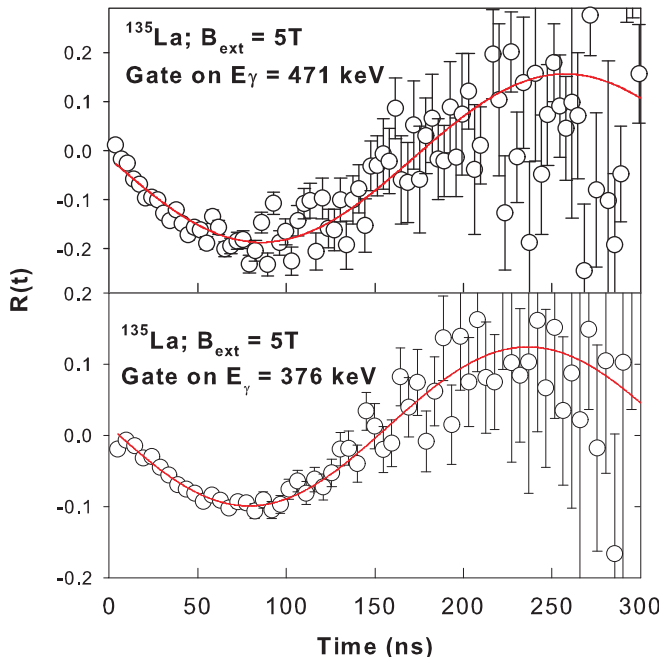


FIG. 3. Spin rotation spectrum of $(23/2^+)$ isomeric state of ^{135}La with $B_{\text{ext}} = 5$ T.

B. Large-scale shell-model calculations

To investigate the level scheme and 2738-keV isomer of ^{135}La microscopically, we performed the large-scale shell-model (LSSM) calculations. The model space is taken as $50 \leq N, Z \leq 82$, namely, it consists of $0g_{7/2}, 1d_{5/2}, 1d_{3/2}, 2s_{1/2}$, and $0h_{11/2}$ single-particle orbits both for protons and neutrons. We adopt the SNBG3 interaction for the neutron-neutron interaction [26] and the N82GYM interaction for the proton-proton interaction [27]. These interactions are determined starting from a G-matrix interaction and χ -square fitted for available experimental data. For the proton-neutron interaction, we adopt the monopole-based universal (V_{MU}) interaction [28] whose central and tensor interactions are scaled by 0.84 and 1.3, respectively, to well reproduce the binding energies and the $11/2^-$ levels in the Sb isotopes [29] and nuclear structure of $N = 80$ isotones [30]. Hereafter, a set of these interactions is called the SNV interaction and is mainly used unless otherwise specified. In some specific cases, we also use the SN100PN interaction [31], which is a G-matrix-based interaction derived from the CD-Bonn nucleon-nucleon potential, for further comparison. The M -scheme dimension of the LSSM calculations reaches 3×10^9 , rather huge. These calculations were performed with the KSHELL code [32] utilizing the Oakforest-PACS supercomputer. We will show the decay scheme to establish the reliability of the present LSSM study, and later, discuss the isomeric character of 2738 keV.

Figure 4 shows the level scheme and the $B(E2)$ transition probabilities of ^{135}La obtained by the LSSM calculations with the SNV interaction. We only show the partial level schemes which correspond to the levels appeared in Fig. 1 of Ref. [33] and Fig. 1 in the present paper. The effective charges are taken as $(e_p, e_n) = (1.6, 0.6)e$ for the computation of the $E2$ matrix elements. We show the $B(E2)$ values larger than $100 e^2\text{fm}^4$ for simplicity in the figure. The measured excited states have been nicely reproduced with the LSSM calculations, including Bands 2, 3, 4, 5, 5a, 6, 7, and 8 shown in Fig. 1 of Ref. [33]. However, the relative position of the $5/2_1^+$ and $7/2_1^+$ states in the reported level scheme is reversed in the calculation.

In Ref. [34], Bands 3, 4, and 5 are identified as favored bands and Band 5a as an unfavored band of Band 5 in the decoupling limit of the particle-rotor model [35]. The present LSSM result supports this interpretation. The configuration of Band 3 is $\pi g_{7/2}$ coupled to the $0^+, 2^+, 4^+, 6^+$ states of ^{134}Ba . Similarly, the configurations of bands 4 and 5 are $\pi g_{5/2}$ and $\pi h_{11/2}$ coupled to the ^{134}Ba ground band, respectively.

Band 2 is interpreted as a $g_{7/2}$ unfavored band built from the $9/2_1^+$ state in the present shell-model study. The $5/2_1^+$ state in Band 2 is also assigned as an unfavored state of $g_{7/2}$, while the $E2$ transition between $5/2_1^+$ state and $9/2_1^+$ state in Band 2 is rather weak. The intensity of the experimental data [33] indicates that the branching ratio of the decay from $9/2_1^+$ state to $5/2_1^+$ state in Band 2 is 15%. This experimental ratio is consistent with that obtained by the shell-model transition probabilities, 11%.

Band 5a is considered to be the unfavored band of the proton $h_{11/2}$ orbit. The large interband $17/2^-$ and $15/2^-$ $E2$ transition is indicated and consistent with the observation of the corresponding γ decay [33]. The branching ratio of the

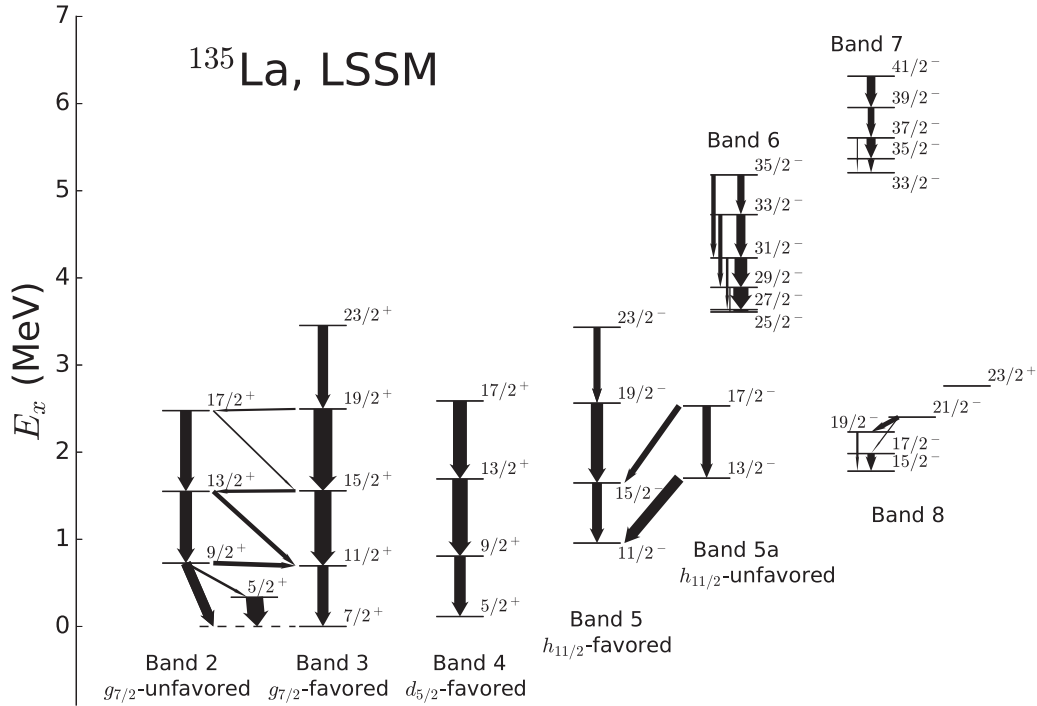


FIG. 4. Level scheme of ^{135}La by the LSSM calculations with the SNV interaction. Arrow width is proportional to the $B(E2)$ value. The labeling of the bands follows the labels of the experimental bands in Ref. [33].

$17/2^-$ state decay to $13/2^-$ is 20% in experiment versus 15% in theory.

Two negative parity dipole bands, Bands 6 and 7, are candidates of the magnetic rotation. According to the LSSM calculations the in-band transitions show large $M1$ probabilities of the order of 1 W.u., which is consistent with the experimentally observed $M1$ characters [33].

Band 8 is not a band in practice, namely no strong inband transition is seen in the LSSM results. The sequence of the decays from the $(23/2_1^+)$ state with excitation energy of 2738 keV occur along the yrast states as experimentally seen in Fig. 2. In Ref. [10], the dipole band with band head energy of 2738 keV was reported and the details of the spin-parity assignments of the states were discussed. The contradictions in spin-parity assignments present in Ref. [33] were solved in Ref. [10] and $(23/2_1^+)$ was assigned to the 2738 keV state.

Figure 5 shows the so-called “ $E2$ map” [36], which was introduced to visualize the complex bands connected by the $E2$ transitions obtained theoretically. It plots the shell-model excitation energy of each positive parity state as a function of the angular momentum I , and the widths of the connected lines show the $B(E2)$ transition probabilities. The three thick $B(E2)$ lines represent two favored and one unfavored bands (band 2, 3, and 4 in Fig. 4), respectively. The experimentally observed $3/2_1^+$ ($E_x = 265$ keV) and $1/2_1^+$ ($E_x = 300$ keV) states [37] most likely correspond to the $d_{5/2}$ unfavored states shown in Fig. 5. Thus, the present LSSM calculation are presented to show its capability to describe the complex band structures of ^{135}La .

Here, we discuss the isomeric property of the experimentally observed 2.738 MeV isomer based on the LSSM. The calculated excitation energy of 2.760 MeV for $23/2^+$ state

is very close to the experimental value of 2.738 MeV. In Fig. 5, the $23/2_1^+$ state has no strong $B(E2)$ transition to the other states, indicating the isomeric property. The shell-model excitation energy of $21/2_1^+$ is 2.932 MeV, which is higher than $23/2^+$ (2.760 MeV) and prohibits the decay to the $21/2_1^+$ state. Another $E2$ -decay possibility from $23/2^+$ is to $19/2^+$ state. It is located at 2.496 MeV, lower than $23/2^+$ level with $B(E2; 23/2_1^+ \rightarrow 19/2_1^+) = 0.5 e^2\text{fm}^4$, which is quite small. Its partial half-life is estimated as 260 ns, much longer than

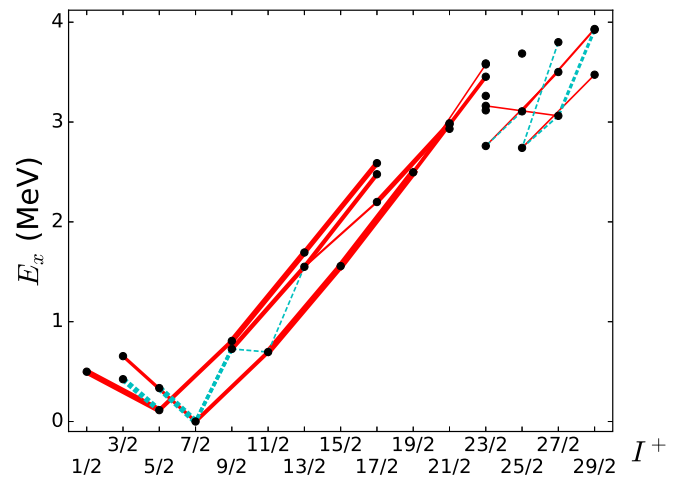


FIG. 5. Excitation energy against the total angular momentum I for positive-parity states of ^{135}La obtained by the LSSM calculations. The widths of the red solid and cyan dashed lines denote the transition probabilities of $B(E2; I+2 \rightarrow I)$ and $B(E2; I+1 \rightarrow I)$, respectively. The $B(E2)$ values larger than $400 e^2\text{fm}^4$ are presented.

TABLE I. Decomposition of the $23/2^+$ states of ^{135}La and the single particle spectroscopic factors C^2S , obtained by the LSSM calculation.

I^π	E_x (MeV)	$^{134}\text{Ba}(10^+) \otimes \pi 1d_{5/2}$	$^{134}\text{Ba}(10^+) \otimes \pi 0g_{7/2}$	$^{134}\text{Ba}(10^+) \otimes \pi 1d_{3/2}$	$^{134}\text{Ba}(7^-) \otimes \pi 0h_{11/2}$
$23/2_1^+$	2.760	0.479	0.073	0.011	0.000
$23/2_2^+$	3.117	0.027	0.131	0.000	0.000
$23/2_3^+$	3.162	0.004	0.078	0.036	0.006
$23/2_4^+$	3.262	0.000	0.001	0.002	0.593

the observed life time of the isomer state, 25.3(3) ns, which is consistent to the expectation of the $E1$ decay to the $21/2_1^-$ state. This small $E2$ value is caused by the difference of the angular-momentum coupling for the $23/2^+$ and $19/2^+$ states: the main configuration of the shell-model $23/2_1^+$ wave function is $(\pi d_{5/2}^1)^{J=5/2} \otimes (\nu h_{11/2}^{-2})^{J=10}$ while the $19/2_1^+$ state is interpreted as a favored state of the $7/2^+$ band, namely, $\pi g_{7/2}$ coupled to the 6^+ state of ^{134}Ba . This wave function brings about rather large g factor of $19/2_1^+$, $g = 0.59$. While $25/2_1^+$ is 2.740 MeV, slightly lower than $23/2_1^+$ 2.760 MeV, it would be reverted in the experiment. If we shift the single-particle energy of $d_{5/2}$ of the SNV interaction so that the ground-state spin becomes $5/2^+$, the $23/2_1^+$ energy gets lower than the $25/2_1^+$ state. The LSSM result with the SN100PN interaction also provides the $23/2_1^+$ level that is lower than $25/2_1^+$. Thus, the $23/2_1^+$ is considered to be the isomeric state, and expected to decay to $21/2_1^-$ with $E1$ transition, while $E1$ transition is strictly forbidden in the present LSSM model space.

To discuss the configuration of the isomer $23/2^+$ state further, we calculated four $23/2^+$ states and their single-particle spectroscopic factors by the LSSM are shown in Table I. The single-particle spectroscopic factor, C^2S , is known to be a good measure to describe nuclear structure. In the table the C^2S of $^{134}\text{Ba}(10^+) \otimes \pi 1d_{5/2} = 23/2_1^+$ shows the largest value among other couplings. It means that the major configuration of $23/2_1^+$ state is $\pi(d_{5/2}) \otimes \nu(h_{11/2})^{-2}$, where the 10^+ state of ^{134}Ba is dominated by the $\nu(h_{11/2})^{-2}$ configuration. With spin g factor quenched 0.64 for protons and 0.74 for neutrons, the shell-model g factor of $23/2_1^+$ is 0.009, small and consistent to the experimental value, $-0.049(3)$. This quenching factor was determined to reproduce available experimental data of $Z = 50$ isotopes and $N = 82$ isotones [26,27]. The calculated g factor of the ground state is 1.32, which is also close to the experimental value, 1.48(4) [18]. If we introduce orbital isovector correction 0.1 to g_l [38], the g factor of the $23/2_1^+$ state is -0.052 and becomes quite close to the experimental value. Since the large occupation of $\nu h_{11/2}$ holes causes the large contribution from neutron orbit to the g factor, the calculated g factor is rather sensitive to the neutron g_l . This isovector correction improves also the ground-state g factor to 1.39, consistently. Thus, the experimentally observed small g factor of $23/2_1^+$ tells us that it is dominated by $\nu h_{11/2}^{-2}$ configuration and consistent with the LSSM result. The result of the SN100PN interaction leads to the same interpretation.

In the present LSSM study, the $\pi h_{11/2}^1 \otimes \nu h_{11/2}^{-1}$ configuration is a minor component, around 2%, in the $23/2_1^+$, $23/2_2^+$, and $23/2_3^+$ wave functions, while Ref. [10] suggested that it is major configuration for the isomer $23/2^+$ state. We found that the shell-model wave function of $23/2_4^+$ at 3.262 MeV is dominated by such proton-excited configuration. Table I shows that the $23/2_4^+$ is dominated by the coupling of $\pi h_{11/2}^1$ and the 7^- state of ^{134}Ba , which has the $\nu d_{3/2}^{-1} h_{11/2}^{-1}$ configuration. The g factor of this state is 0.52 and apparently disagrees with the experimental value.

IV. CONCLUSION

The precision g -factor measurement for the 2738 keV isomer in ^{135}La has been carried out using TDPAD method. The measured g -factor value for this isomer has been found to be $-0.049(3)$. Large-scale shell-model calculations have been performed to calculate the level structure of ^{135}La as well as to understand the configuration of the measured isomer at 2738 keV excitation energy. The shell-model results provide an excellent description of the measured level scheme. In particular, the shell-model result on the g factor of the $23/2^+$ isomer is very close to the measured g factor of $-0.049(3)$. As a consequence, the $23/2^+$ state of ^{135}La has been identified as $^{134}\text{Ba}(10_1^+) (\nu 0h_{11/2}^{-2})$ and proton $1d_{5/2}$ configuration by the LSSM study.

ACKNOWLEDGMENTS

The authors acknowledge the TIFR-BARC Pelletron Linac Facility for providing good quality beam. The help and cooperation from S. M. Davane, B. Naidu, S. Jadhav, and R. Donthi for setting up the experimental apparatus is acknowledged. This work is partially supported by the International Joint Research Promotion Program of Osaka University. Authors thank Prof. C. M. Petrache for useful discussion at RCNP, Osaka University. N.S. and Y.U. acknowledge priority issue 9 to be tackled by using Post K Computer (hp170230, hp180179), Interdisciplinary Computational Science Program in CCS, University of Tsukuba, KAKENHI (Grants No. 17K05433 and No. 15K05094), and CNS-RIKEN joint project for large-scale nuclear structure calculations. We acknowledge M. Honma for the collaborations and N82GYM and SNBG3 interactions.

[1] H. Nishibata, R. Leguillon, A. Odahara, T. Shimoda, C. M. Petrache, Y. Ito, J. Takatsu, K. Tajiri, N. Hamatani,

R. Yokoyama, E. Ideguchi, H. Watanabe, Y. Wakabayashi, K. Yoshinaga, T. Suzuki, S. Nishimura, D. Beaumel, G. Lehaut,

- D. Guinet, P. Desesquelles, D. Curien, K. Higashiyama, and N. Yoshinaga, *Phys. Rev. C* **91**, 054305 (2015).
- [2] C. M. Petrache, R. A. Bark, S. T. H. Murray, M. Fantuzzi, E. A. Lawrie, S. Lang, J. J. Lawrie, S. M. Maliage, D. Mengoni, S. M. Mullins, S. S. Ntshangase, D. Petrache, T. M. Ramashidzha, and I. Ragnarsson, *Phys. Rev. C* **74**, 034304 (2006).
- [3] A. Vogt *et al.*, *Phys. Rev. C* **95**, 024316 (2017).
- [4] J. Genevey, J. A. Pinston, C. Foin, M. Rejmund, R. F. Casten, H. Faust, and S. Oberstedt, *Phys. Rev. C* **63**, 054315 (2001).
- [5] J. Genevey *et al.*, *Eur. Phys. J. A* **9**, 191 (2000).
- [6] J. Genevey, J. A. Pinston, H. R. Faust, R. Orlandi, A. Scherillo, G. S. Simpson, I. S. Tsekhanovich, A. Covello, A. Gargano, and W. Urban, *Phys. Rev. C* **67**, 054312 (2003).
- [7] H. Watanabe, G. J. Lane, G. D. Dracoulis, A. P. Byrne, P. Nieminen, F. G. Kondev, K. Ogawa, M. P. Carpenter, R. V. F. Janssens, T. Lauritsen, D. Seweryniak, S. Zhu, and P. Chowdhury, *Phys. Rev. C* **79**, 064311 (2009).
- [8] S. Biswas, R. Palit, A. Navin, M. Rejmund, A. Bisoi, M. S. Sarkar, S. Sarkar, S. Bhattacharyya, D. C. Biswas, M. Caamano, M. P. Carpenter, D. Choudhury, E. Clement, L. S. Danu, O. Delaune, F. Farget, G. deFrance, S. S. Hota, B. Jacquot, A. Lemasson, S. Mukhopadhyay, V. Nanal, R. G. Pillay, S. Saha, J. Sethi, P. Singh, P. C. Srivastava, and S. K. Tandel, *Phys. Rev. C* **93**, 034324 (2016).
- [9] T. Alharbi, P. H. Regan, N. Marginean, Z. Podolyak, O. J. Roberts, A. M. Bruce, N. Alkhomashi, R. Britton, D. Bucurescu, D. Deleanu, D. Filipescu, D. Ghita, T. Glodariu, C. Mihai, K. Mulholland, R. Lica, R. Marginean, M. Nakhostin, A. Negret, C. R. Nita, L. Stroe, T. Sava, C. Townsley, and N. V. Zamfir, *Phys. Rev. C* **91**, 027302 (2015).
- [10] R. Leguillon, H. Nishibata, Y. Ito, C. M. Petrache, A. Odahara, T. Shimoda, N. Hamatani, K. Tajiri, J. Takatsu, R. Yokoyama, E. Ideguchi, H. Watanabe, Y. Wakabayashi, K. Yoshinaga, T. Suzuki, S. Nishimura, D. Beaumel, G. Lehaut, D. Guinet, P. Desesquelles, D. Curien, A. Astier, T. Konstantinopoulos, and T. Zerrouki, *Phys. Rev. C* **88**, 044309 (2013).
- [11] A. Vancraeynest, C. M. Petrache, D. Guinet, P. T. Greenlees, U. Jakobsson, R. Julin, S. Juutinen, S. Ketelhut, M. Leino, M. Nyman, P. Peura, P. Rahkila, P. Ruotsalainen, J. Saren, C. Scholey, J. Sorri, J. Uusitalo, P. Jones, C. Ducoin, P. Loutesse, C. Mancuso, N. Redon, O. Stezowski, P. Désesquelles, R. Leguillon, A. Korichi, T. Zerrouki, D. Curien, and A. Takashima, *Phys. Rev. C* **87**, 064303 (2013).
- [12] J. J. Valiente-Dobon *et al.*, *Phys. Rev. C* **69**, 024316 (2004).
- [13] Müller-Veggian *et al.*, *Z. Phys. A* **290**, 43 (1979).
- [14] Müller-Veggian *et al.*, *Nucl. Phys. A* **304**, 1 (1978).
- [15] Müller-Veggian *et al.*, Annual Report 1979, IKP-KFA Jülich, Jül-Spez-72 (1980).
- [16] T. Morek *et al.*, *Z. Phys. A* **298**, 267 (1980).
- [17] M. Ohshima *et al.*, *Hyperfine Interact.* **7**, 103 (1979).
- [18] N. J. Stone, *At. Data Nucl. Data Tables* **90**, 75 (2005).
- [19] A. I. Levon, O. F. Nemets, V. A. Stepanenko, and V. P. Chepak, *Izv. Akad. Nauk SSSR, Ser. Fiz.* **40**, 1249 (1976) [*Bull. Acad. Sci. USSR, Phys. Ser.* **40**, 125 (1976)].
- [20] N. Bansal *et al.*, *Proc. DAE Symp. Nucl. Phys.* **59**, 68 (2014).
- [21] J. Goto, M. Tanigaki, A. Taniguchi, Y. Ohkubo, Y. Kawase, S. Ohya, K. Nishimura, T. Ohtsubo, and S. Muto, *J. Phys. Soc. Jpn.* **72**, 723 (2003).
- [22] S. N. Mishra, S. K. Mohanta, S. M. Davane, N. Kulkarni, and P. Ayyub, *Phys. Rev. Lett.* **105**, 147203 (2010).
- [23] S. K. Mohanta, S. N. Mishra, Kartik K. Iyer, and E. V. Sampathkumaran, *Phys. Rev. B* **87**, 125125 (2013).
- [24] S. Saha, S. K. Mohanta, Sayani Biswas, R. Palit, and S. N. Mishra, *Hyperfine Interact.* **237**, 121 (2016).
- [25] N. Xu, Ph.D. thesis, State University of New York, New York 1990.
- [26] M. Honma, T. Otsuka, T. Mizusaki, and M. Hjorth-Jensen, *RIKEN Accel. Progr. Report* **45**, 35 (2011).
- [27] M. Honma, T. Otsuka, T. Mizusaki, and M. Hjorth-Jensen, *RIKEN Accel. Progr. Report* **49**, 77 (2015).
- [28] Y. Utsuno, T. Otsuka, B. A. Brown, M. Honma, T. Mizusaki, and N. Shimizu, *Phys. Rev. C* **86**, 051301(R) (2012).
- [29] Y. Utsuno, T. Otsuka, N. Shimizu, M. Honma, T. Mizusaki, Y. Tsunoda, and T. Abe, *Euro. Phys. J. Web Conf.* **66**, 02106 (2014).
- [30] C. M. Petrache *et al.* (unpublished).
- [31] B. A. Brown, N. J. Stone, J. R. Stone, I. S. Towner, and M. Hjorth-Jensen, *Phys. Rev. C* **71**, 044317 (2005).
- [32] N. Shimizu, [arXiv:1310.5431](https://arxiv.org/abs/1310.5431).
- [33] R. Garg, S. Kumar, M. Saxena, S. Goyal, D. Siwal, S. Verma, R. Palit, S. Saha, J. Sethi, S. K. Sharma, T. Trivedi, S. K. Jadav, R. Donthi, B. S. Naidu, and S. Mandal, *Phys. Rev. C* **87**, 034317 (2013).
- [34] J. Chiba, R. Hayano, M. Sekimoto, H. Nakayama, and K. Nakai, *J. Phys. Soc. Jpn.* **43**, 1109 (1977).
- [35] P. Ring and P. Schuck, *The Nuclear Many-Body Problem* (Springer-Verlag, New York/Heidelberg/Berlin, 1980).
- [36] B. A. Brown and W. D. M. Rae, *Nucl. Data Sheets* **120**, 115 (2014).
- [37] Y. Nagai and K. Hisatake, *J. Phys. Soc. Jpn.* **36**, 1501 (1974).
- [38] M. Honma, T. Otsuka, B. A. Brown, and T. Mizusaki, *Phys. Rev. C* **69**, 034335 (2004).